Structural Basis of Antibody Cross-Reactivity: Solution Conformation of an Immunogenic Peptide Fragment Containing both T and B Epitopes

Philippe Cuniasse,*,‡ Aline Thomas,§,|| Jeremy C. Smith,§ Hung Lam Thanh,‡ Michel Léonetti,‡ and André Ménez‡

CEA, Département d'Ingénierie et d'Etudes des Protéines, and CEA, Section de Biophysique des Protéines et des Membranes, Département de Biologie Cellulaire et Moléculaire, C. E. Saclay, 91191 Gif-sur-Yvette Cedex, France

Received January 23, 1995; Revised Manuscript Received July 5, 1995[⊗]

ABSTRACT: A synthetic octadecapeptide with the amino acid sequence of residues 23−40 of toxin α from *Naja nigricollis*, cyclized with a disulfide bridge between residues 23 and 40, induces antibodies that cross-react with toxin α. We report a structural analysis of this peptide in aqueous solution using NMR spectroscopy and molecular modeling. Structures compatible with the 151 obtained NMR distance restraints were generated using a random simulated annealing protocol followed by restrained high-temperature dynamics and energy minimization. The generated structures are compared with that of the corresponding sequence in the native toxin. The two stretches 23−28 and 37−40 adopt a canonical β-strand structure in the toxin but are disordered in the peptide. The region 28−36 is ordered in both the peptide and the toxin. Residues 28−30 and 34−36 adopt β-strand structures in the toxin but loop structures in the peptide. Residues 30−33 form a reverse turn in both the peptide and the toxin. Residues Val-27, Trp-28, Ile-35, and Ile-36 form a hydrophobic cluster. The similar, reverse-turn fold of residues 30−33 in the peptide and the toxin may be associated with the immunogenic cross-reactivity.

For two decades synthetic peptides have been used in the field of immunology with a view to designing new vaccination strategies (Steward et al., 1987; Arnon, 1991). Some synthetic peptides are capable of eliciting antibodies that recognize not only the peptide but also folded proteins possessing the same amino acid sequences (Arnon & Sela, 1969; Arnon et al., 1971; Lerner, 1982; Lerner et al., 1984). In many cases, however, antibodies raised against linear peptides derived from portions of native protein sequences exhibit poor affinities for the native protein and therefore have weak protecting capacities (Palmenberg, 1987; Jemmerson, 1987). This problem can sometimes be overcome, and the recognition of the parent protein by the synthetic peptide improved, by introducing conformational restrictions on the peptide (Arnon & Sela, 1969; Arnon et al., 1971). The questions therefore arise as to whether the cross-reactivity is associated with a conformational similarity between the peptide fragment and the cognate sequence in the native protein and whether a conformational similarity is detectable in the peptide in aqueous solution.

In previous work it was shown that the region 23−40 of toxin α of the venom of the African spitting cobra *Naja nigricollis* contains part of the B epitope for the protein (Trémeau et al., 1986). Antibodies raised against the linear peptide with the same sequence (23−40) have a weak cross-reactivity with the native protein (Léonetti et al., 1990; Léonetti, unpublished results). In the toxin residues 23−40 form a β-hairpin motif consisting of two strands of β-sheet (residues 23−29 and 34−40) and a Type I β-turn (residues 30−33) (Zinn-Justin et al., 1992). Residues Cys-23 and Cys-40 are separated by almost 4 Å in the toxin but are not disulfide-bonded. The immunization of BALB/c mice with the synthetic octadecapeptide cyclized with a disulfide bond between Cys-23 and Cys-40 raises antibodies that recognize the parent protein, toxin α (Léonetti et al., 1990). The presence of the disulfide bond might be expected to bias the configurational distribution of the peptide toward that of the native protein.

Anti-peptide antisera are usually raised in animals by injecting the peptide coupled to a carrier protein. It has been shown that the presence of the carrier molecule can influence the specificity of the antibodies raised against the peptide (Bahraoui et al., 1986). This suggests that the conformation and/or accessibility of the peptide can be influenced by the carrier. Free peptides, *i.e.*, not coupled to a carrier protein, can sometimes elicit an immune response (Dreesman et al., 1982; DiMarchi et al., 1986). It has been shown that the requirement for this is that the free peptide should possess a T epitope (Leclerc et al., 1987; Good et al., 1987; Francis et al., 1987). The T epitope can be either linearly fused to the B epitope-containing synthetic peptide (Leclerc et al., 1987; Good et al., 1987; Borras-Cuesta et al., 1987) or directly incorporated within the B epitope (Roy et al., 1989; Léonetti et al., 1990). The present cyclic peptide has the capacity to stimulate T cells in BALB/c mice (Léonetti et al., 1990). This allows its injection free of coupling, thereby avoiding the necessity of a protein carrier in the selection of anti-peptide antibodies. Consequently, the structural analysis of the peptide in aqueous solution appears particularly appropriate for an investigation of the role of conformation in immunogenic cross-reactivity between a peptide fragment and its corresponding native protein.

Although oligopeptides can possess considerable conformational flexibility in aqueous solution, some have been shown to exhibit secondary structural preferences (Dyson et al., 1985, 1988a; Wright et al., 1988). Helical structure

* To whom correspondence should be addressed.
‡ Département d'Ingénierie et d'Etudes des Protéines.
§ Section de Biophysique des Protéines et des Membranes, Département de Biologie Cellulaire et Moleculaire.
|| Present address: Institut de Biologie Structurale, 41 Avenue des Martyrs, 38027 Grenoble Cedex, France.
⊗ Abstract published in *Advance ACS Abstracts,* September 1, 1995.

0006-2960/95/0434-12782$09.00/0

has been found in peptide fragments with sequences of helical regions of native proteins (Rico et al., 1983; Goodman & Kim, 1989) and reverse turns have also been observed (Williamson et al., 1986; Dyson et al., 1988b, 1990; Reed et al., 1988; Delepierre et al., 1990; Blanco et al., 1991, 1993). Recently, several peptide fragments were shown to possess reverse turns in solution at the same sequence location as in the corresponding native proteins (Sönnichsen et al., 1992; Shin et al., 1993; Blanco et al., 1994), although for many peptides the turns found have been at different places.

To investigate the configurational distribution of peptide 24-41c[1] in aqueous solution we have performed ^{1}H NMR[2] spectroscopy experiments. Structures compatible with the NMR data were derived using a simulated annealing protocol and refined by high-temperature restrained molecular dynamics and energy minimization. The comparison of the structures of the peptide and the corresponding sequence in the native protein provides insight into the role of conformation in the cross-reactivity of the antibodies raised against the peptide.

MATERIALS AND METHODS

The sequence of the chemically synthesized cyclic peptide 24-41c is as follows: NH_2-Cys23-Tyr24-Lys25-Lys26-Val27-Trp28-Arg29-Asp30-His31-Arg32-Gly33-Thr34-Ile35-Ile36-Glu37-Arg38-Gly39-Cys40-$CONH_2$ with a disulfide between Cys-23 and Cys-40 (Leonetti et al., 1990).

NMR Experiments. Samples of the peptide were prepared at a concentration of 7 mM in ^2H_2O and 90% ^1H_2O/10% ^2H_2O. The pH was adjusted to 5.4. No correction for the isotope effect was applied to the pD of the sample in ^2H_2O. The chemical shifts were measured relative to the internal reference, sodium 2,2,3,3-tetradeutero-3-(trimethylsilyl)propionate (TSP).

NMR spectra were recorded on Bruker AMX500 and AMX600 spectrometers at 276 K. All spectra were collected with quadrature detection in t_2. NOESY spectra were recorded in the phase-sensitive mode (Bodenhausen et al., 1984) with 350- and 80-ms mixing times. Quadrature detection in t_1 was performed using time-proportional phase incrementation (Marion & Wüthrich, 1983). NOESY spectra were recorded with 4096 data points in the t_2 dimension. A total of 512 free induction decays were collected in the t_1 dimension. After zero-filling to give a 4096 × 4096 matrix, a 90° phase-shifted sine bell was applied in both dimensions prior to Fourier transformation. The ^1H_2O resonance was suppressed by applying a 1-1 observation pulse to avoid loss of signal of the amide protons due to exchange with the solvent (Plateau & Gueron, 1982). The NMR data were processed with the Bruker UXNMR software on a Bruker X32 workstation and with the Felix 2.1 software (Biosym Technologies Inc.) on a Silicon Graphics 4D35 workstation.

A ROESY spectrum (Bothner-By et al., 1985) was recorded in the hypercomplex format (States et al., 1982) with a 100-ms mixing time using a continuous wave for isotropic mixing (Bax & Davis, 1985). A TOCSY spectrum in ^1H_2O was recorded in the hypercomplex format using a 1-1 observation pulse (Bax et al., 1987) and a 120-ms mixing time. Isotropic mixing was performed with a Waltz 16 sequence sandwiched between 2.5-ms trim pulses. A COSY spectrum (Aue et al., 1976) in 90% ^1H_2O/10% ^2H_2O was recorded in the phase-sensitive mode. A total of 4096 data points in t_2 were measured for a spectral width of 7575 Hz, and 512 free induction decays were collected in the t_1 dimension. After zero-filling to give a 8192 × 2048 matrix, a shifted sine bell was applied in both dimensions prior to Fourier transformation. This gave a resolution of 1.8 Hz in the $F2$ dimension.

The temperature dependences of all the NH proton chemical shifts were determined by recording a series of COSY spectra at temperatures between 276 and 303 K. This magnitude-mode COSY experiment was recorded using a four-step phase cycle (without removal of quadrature images) to reduce the acquisition time.

Interproton distance restraints were obtained from analysis of the 80-ms mixing time NOESY spectrum and the 100-ms mixing time ROESY spectrum of the peptide. The distances were calculated by integration of the NOESY or ROESY cross-peaks. The σ_{ref}/σ_{ij} were estimated using the ratio of the intensity of the NOE (or ROE) between the protons i and j to the NOE between two protons for which the distance is known and fixed. The geminal protons Hα/Hα′ of glycine, for which the distance is 1.78 Å, was used as the reference. It has been shown that using a geminal pair of protons as a reference leads to an underestimation of the calculated distances due to the angular fluctuations of the geminal reference pair, reducing the apparent cross-relaxation rate (Brüschweiler et al., 1992). As a result, the rates for other proton pairs appear to be correspondingly larger. To take this effect into account, a factor of 0.5 Å was added to the estimated distances.

It was not possible to integrate all the correlations observed in the 350-ms NOESY spectrum in the 80-ms mixing time NOESY and the 100-ms mixing time ROESY spectra due to the poor signal-to-noise ratio in these experiments. Therefore, certain distances (~30%) were obtained by semiquantitative analysis of the 350-ms mixing time NOESY spectrum in which integrated intensities were grouped into four classes. These classes were assigned maximum distances of 2.5, 2.8, 3.5, and 5.0 Å.

The values of the $^3J_{NH-H_\alpha}$ obtained from analysis of the phase-sensitive COSY spectrum allowed the unambiguous determination of six ϕ angles, estimated from the Karplus curve (Karplus, 1959; Bystrov, 1976). Further χ_1 angles were estimated from the $^3J_{H_\alpha H_\beta}$ and $^3J_{H_\alpha H_{\beta'}}$ coupling constants and from the $H_\alpha-H_\beta$ and $H_\alpha-H_{\beta'}$ NOEs.

Molecular Modeling. Structures compatible with the experimental distance restraints obtained from the analysis of the NOESY/ROESY experiments and from the ϕ and χ_1 dihedral angle restraints were generated using a procedure of simulated annealing (Nilges et al., 1988) written in X-PLOR version 3.1 (Brünger et al., 1987; Brünger, 1992). The distance restraints (r_{ij}) were incorporated in the total potential energy using a square-well function (Brünger, 1992). To take into account the uncertainty in the distances,

[1] The peptide is designated as 24-41c in the text. This sequence numbering is that currently used for short-chain curaremimetic toxins possessing 62 residues, such as erabutoxins. The sequence 24-41c corresponds to residues 23−40 of the toxin α.

[2] *Abbreviations*: COSY, two-dimensional correlated spectroscopy; NMR, nuclear magnetic resonance; NOE, nuclear Overhauser effect; NOESY, two-dimensional nuclear Overhauser spectroscopy; ROE, rotating-frame nuclear Overhauser effect; ROESY, two-dimensional rotating-frame nuclear Overhauser spectroscopy; TOCSY, two-dimensional total correlation spectroscopy; RMS, root mean square.

the upper bounds in the restraint terms were set at $1.2r_{ij}$. The ϕ and χ_1 torsion angle restraints were included using a biharmonic potential with a flat minimum extended ± 20° from the experimental values. A total of 151 experimental distance restraints were included: 87 intraresidue, 53 sequential interresidue, 8 medium-range ($i \rightarrow [i + 2, i + 5]$, where i refers to the residue number), and 3 long-range restraints ($i \rightarrow [i + 5, ...]$, together with 13 experimental torsion angle restraints (6 ϕ and 7 χ_1).

The random simulated annealing protocol was run using the parmallhdg force field of X-PLOR version 3.1. The potential energy function contains bond, angle, improper torsion angle, nonbonded interactions, distance restraint terms (force constant k_{DR}), and experimental ϕ and χ_1 dihedral angle restraint terms (force constant k_{EDR}). During the random simulated annealing stage, the nonbonded interactions were treated using a purely repulsive potential. Coulombic interactions were not included. The temperature was maintained by strong coupling to a thermal bath (Berendsen et al., 1984).

Starting from random positions of the atoms of the molecule, initial structures were subjected to 500 steps of minimization and followed by 2.5 ps of restrained molecular dynamics (k_{DR} = 0.1 kcal mol^{-1} Å^{-2} and k_{EDR} = 0.1 kcal mol^{-1} rad^{-2}) at 1000 K. The resulting structures were submitted to 4.5 ps of simulated annealing from 1000 to 100 K. During this stage the distance restraints force constant (k_{DR}) and the experimental dihedral restraints force constant (k_{EDR}) were linearly increased from 0.1 to 50 kcal mol^{-1} Å^{-2} and 0.1 to 50 kcal mol^{-1} rad^{-2}, respectively, and the van der Waals radii were linearly increased to reach their paramallhdg values at the end of the cooling. The simulated annealing was followed by 500 steps of energy minimization.

The resulting structures were submitted to 3 ps of high-temperature restrained molecular dynamics at 600 K (integration step 0.5 fs) and minimized, using the CHARMM22 force field of the XPLOR version 3.1 software. The potential contained terms corresponding to bond stretching, angle bending, dihedral angle twisting, improper torsion angle bending, nonbonded interactions, and experimental distance and dihedral angle restraints. The nonbonded interactions were represented by a Lennard-Jones potential for van der Waals interactions and a coulombic electrostatic term. All calculations were carried out without explicit water molecules. The electrostatic screening effect of the solvent was represented approximately by setting the relative dielectric constant equal to the distance between the atoms concerned and by making the charged side chains neutral, except for Asp-30, as this residue was found to participate to an intramolecular hydrogen bond.

This protocol (random simulated annealing followed by high-temperature molecular dynamics and minimization in the CHARMM 22 force field) was repeated 25 times in order to obtain a set of structures compatible with the experimental restraints. The 10 best structures, each having a distance restraints energy < 2 kcal mol^{-1} Å^{-2}, were analyzed.

The calculations were carried out on a SGI Challenge computer. The structures were visualized on an Indigo SGI workstation and program Sybyl (Tripos Associates Inc.).

RESULTS

NMR Experiments. The assignment of the amide and side-chain proton resonances of the peptide 24-41c was made using the standard approach (Wüthrich et al., 1983). Val-27, Thr-34, Ile-35, and Ile-36 were expected to give rise to the most intense resonances in the low-field region of the one-dimensional ^{1}H NMR spectrum. Three intense cross-peaks are observed at 0.78, 0.95, and 1.18 ppm. The 1.18 ppm resonances can be assigned to the methyl group of Thr-34, for which the deshielding effect of the β-OH group induces a downfield shift compared to the methyl resonances of valine. This was the starting point for the sequential resonance assignment. All amide and side-chain proton resonances were unambiguously assigned from TOCSY and NOESY spectra except the exchangeable lysine NH$^{\delta 2}$, arginine NH$^{\eta 1}$, arginine NH$^{\eta 2}$, and histidine HN$^{\delta 1}$ protons. The CH2$^{\gamma}$ and CH3$^{\delta}$ proton resonances of the isoleucines were assigned by examination of both the COSY and the TOCSY spectra. The chemical shifts of all assigned proton resonances are listed in Table 1.

Table 1: Chemical Shifts of the Proton Resonances of Peptide 24−41c[a]

residue	HN	Hα	Hβ	other
Cys-23		4.34	3.28, 3.28	
Tyr-24	9.00	4.74	3.00, 3.05	Cδ12 7.15
				Cε12 6.83
Lys-25	8.50	4.30	1.65, 1.72	Cγ H 1.25, 1.25
				Cδ H 1.40, 1.40
				Cε H 2.97, 2.97
Lys-26	8.33	4.43	1.60, 1.75	Cγ H 1.25, 1.25
				Cδ H 1.30, 1.30
				Cε H 2.79, 2.79
Val-27	8.37	4.54	2.03	Cγ H 0.92
Trp-28	8.90	4.83	3.21, 3.28	Cβ1H 7.16
				Cε3H 7.53
				Cζ3H 7.19
				Cη2H 7.05
				Cζ2H 7.45
				NHε1 10.22
Arg-29	8.40	4.79	1.61, 1.65	Cγ H 1.42, 1.42
				Cδ H 3.12, 3.12
				NHε 7.27
Asp-30	8.49	4.56	2.70, 3.14	
His-31	8.63	4.53	3.32, 3.32	Cε1H 7.25
				Cδ2H 7.47
Arg-32	8.22	4.35	1.86, 1.90	Cγ H 1.38, 1.50
				Cδ H 3.08, 3.13
				NHε 7.36
Gly-33	8.28	4.20, 3.75		
Thr-34	8.38	4.28	4.12	Cγ H 1.18
Ile-35	8.63	4.23	1.78	Cγ1H 1.10
				Cγ2H 0.82
				Cδ H 0.82
Ile-36	8.75	4.25	1.55	Cγ1H 1.12
				Cγ2H 0.78
				Cδ H 0.75
Glu-37	8.48	4.60	1.97, 2.0	Cγ H 2.21, 2.25
Arg-38	8.78	4.55	1.78, 1.92	Cγ H 1.60, 1.65
				Cδ H 3.13, 3.13
				NHε 7.16
Gly-39	8.71	4.06, 4.06		
Cys-40	8.70	4.75	3.04, 3.35	

[a] Chemical shifts were determined at 276 K, pH 5.4, and are given in parts per million relative to the internal reference TSP. ND: not determined.

The following observations are consistent with the presence of structure in the peptide under the experimental conditions: (i) the Hα and/or HN proton resonances of several residues possess a downfield shift relative to their random coil values (Wüthrich, 1986); (ii) a distinct chemical shift pattern was found for each of the three arginines, the

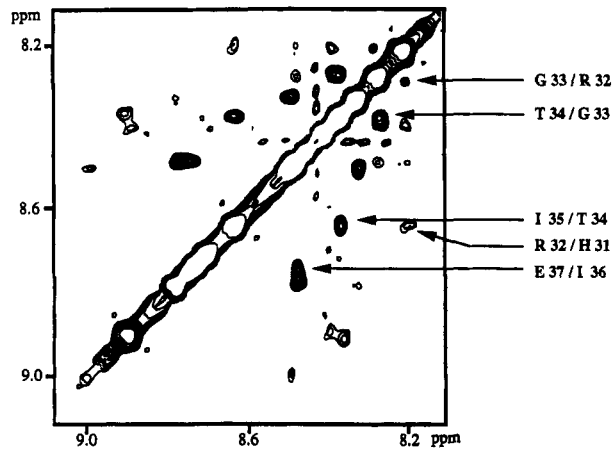

FIGURE 1: Expanded contour plot of the NH−NH region of the 350-ms mixing time NOESY spectrum of the peptide 24-41c recorded in ^1H_2O at 276 K.

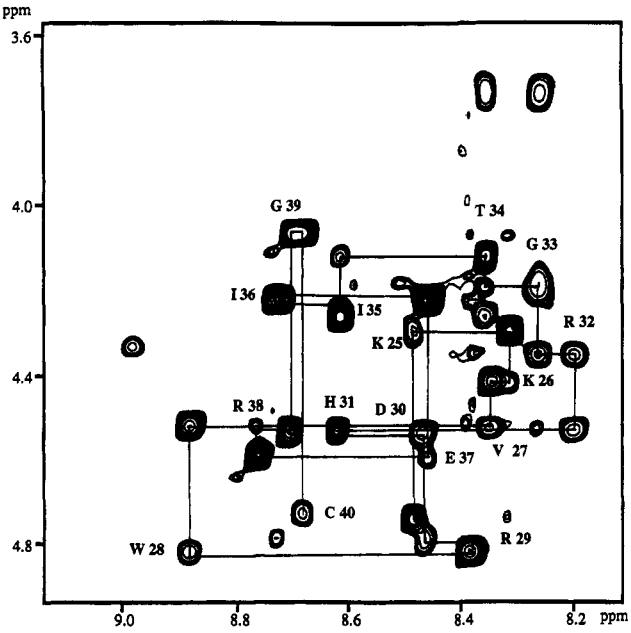

FIGURE 2: Expanded contour plot of the NH−Hα region of the 350-ms mixing time NOESY spectrum of the peptide 24-41c recorded in ^1H_2O at 276 K. The sequential connectivities are shown from residue Tyr-24 to residue Cys-40.

two lysines, and the two isoleucines; and (iii) the Hα/Hα′ proton resonances of Gly-33 exhibit nonequivalent chemical shifts.

Several pieces of evidence suggest that the residues 30−33 form a reverse turn. The NH/NH region of the NOESY spectrum (Figure 1) shows an NOE cross-peak between the His-31 NH and Arg-32 NH proton resonances and between the Arg-32 NH and Gly-33 NH proton resonances. Furthermore, the Hα/NH region of the NOESY spectrum (Figure 2) shows an NOE cross-peak between the Gly-33 NH and the His-31 Hα proton resonances. However, the determination of the turn type is not unambiguous since both dαN(31,32) and dNN(31,32) cross-peaks are observed; the former effect is typical for a Type II turn whereas the latter characterizes a Type I turn. These data could be explained by assuming either a Type I/Type II equilibrium in fast exchange on the NMR time scale or a noncanonical reverse turn. The low value observed for the temperature coefficient of the Gly-33 NH proton resonance (−1.5 ppb K^{-1}) is also

Table 2: Experimental Values of the Temperature Coefficients, Coupling Constants, and χ_1 Angles of the Hα Proton Resonances of Each Residue of the Peptide 24−41c[a]

residue	$-\Delta\delta/\Delta T$ (ppb K^{-1})	$^3J_{NH-H\alpha}$ (Hz)	χ_1 (deg)
Cys-23		ND	
Tyr-24	8.0	10.5	ND
Lys-25	ND	8	
Lys-26	3.0	7.5	180
Val-27	6.4	8	
Trp-28	6.3	9	60
Arg-29	6.8	ND	60
Asp-30	3.6	9	60
His-31	5.9	7.5	ND
Arg-32	ND	8.5	180
Gly-33	1.5	12/ND[b]	
Thr-34	4.4	7	
Ile-35	6.7	7	
Ile-36	5.5	11	
Glu-37	5.1	11	−60
Arg-38	5.4	7	180
Gly-39	6.7	ND	
Cys-40	7.3	7.5	−60

[a] As determined from analysis of the $^3J_{H\alpha-H\beta}$ and $^3J_{H\alpha-H\beta'}$ coupling constants and $d_{\alpha\beta}$ and $d_{\alpha\beta'}$ nOe's. ND: not determined. [b] $^3J_{NH-H\alpha}$ and $^3J_{NH-H\alpha'}$.

consistent with the presence of a turnlike structure involving residues Asp-30, His-31, Arg-32, and Gly-33 (see Table 2).

Another interesting observation concerns the presence of a cross-peak between the Ile-36 NH and Arg-29 Hα proton resonances (Figure 2), indicating that these two residues are in spatial proximity. Additional NOEs (Gly-33 NH/Arg-29 (Hβ, Hγ, Hδ), Trp-28 Cε3H/Ile-36 Hβ, Trp28 Cε3H/Ile-36 CβH, Trp-28 Cξ2H/Ile-36 CδH, and Trp-28 Cξ3H/Ile-36 CδH) are also consistent with the presence of structure in this part of the peptide. The observation of sequential dNN connectivities between residues Gly-33/Thr-34 and Thr-34/Ile-35 (Figure 2) indicates that the reverse turn structure is not followed by a β-sheet strand. Finally, examination of the peptide χ_1 angles (Table 2) shows that the positions of some side chains relative to the backbone are well-defined.

Molecular Modeling. It is well recognized that the connectivities observed in cross-relaxation experiments for peptides in aqueous solution may arise from a single conformation or from more than one in rapid exchange on the NMR time scale. The qualitative analysis of the NOEs in the peptide 24-41c indicated that there was no necessity to consider *a priori* multiple conformations to explain the data. Therefore, the whole data set was used to generate a set of 25 structures using the simulated annealing protocol followed by high-temperature restrained molecular dynamics and energy minimization as described in Materials and Methods. The 10 best structures, each having distance restraints energy lower than 2 kcal mol^{-1} $Å^{-2}$, were analyzed. Taking into account the 20% uncertainty, no distance restraints violation > 0.1 Å was observed in the 10 structures. Furthermore, taking into account the 20° uncertainty, no violation > 2° of the experimental ϕ and χ_1 torsion angle restraints was observed. The average refinement parameters calculated from the 10 best refined structures (average restraint violations, average energetic contributions, and mean pairwise RMS differences) of the 10 structures analyzed are reported in Table 3. The average pairwise RMS difference among the 10 structures calculated for the backbone heavy atoms of residues 23−40 is 3.91 Å (Table 3). However, the corresponding average RMS difference for residues 28−

Table 3: Mean Parameters Calculated from the 10 Best Refined Structures[a]

$\langle V_{noe} \rangle^b$	0.0138 (±0.00286)
$\langle V_{cdih} \rangle^c$	0.94 (±0.47)
$\langle E_{pot} \rangle^d$	−213 (±12.2)
$\langle E_{bond} \rangle$	22.1 (±0.7)
$\langle E_{angl} \rangle$	58.6 (±4.2)
$\langle E_{dihe} \rangle$	82.7 (±5.7)
$\langle E_{impr} \rangle$	2.09 (±0.7)
$\langle E_{vdW} \rangle$	25.9 (±6.7)
$\langle E_{elec} \rangle$	−406.9 (±9.5)
$\langle E_{noe} \rangle$	1.45 (±0.5)
$\langle E_{cdih} \rangle$	0.19 (±0.18)
⟨pRMSD all⟩[e]	3.91 (±0.94)
⟨pRMSD 28−36⟩[e]	1.36 (±0.37)

[a] Standard deviations are given in parentheses. [b] Average violation of the distance restraints in angstroms. [c] Average violation on the dihedral ϕ and χ^1 restraints in degrees. [d] Average potential energy contributions in kilocalories per mole. E_{pot}, total; E_{bond}, bond stretching energy; E_{angl}, angle bending; E_{dihe}, dihedral torsion angle twisting; E_{impr}, improper torsion angle twisting; E_{vdW}, van der Waals; E_{elec}, electrostatic, E_{noe}, experimental distance restraints energy; E_{cdih}, experimental torsion angle (ϕ and χ_1) energy. The cyclic peptide contains 309 atoms, 312 bonds, 556 valence angles, 832 dihedral angles, and 45 improper angles. There were 151 distance restraints and 13 dihedral angle restraints. [e] Average pairwise RMS differences of the backbone atom coordinates (N, Cα, and C) for all residues of the peptide 24−41c (⟨pRMSD all⟩) and for residues 28−36 of the peptide (⟨pRMSD 28−36⟩).

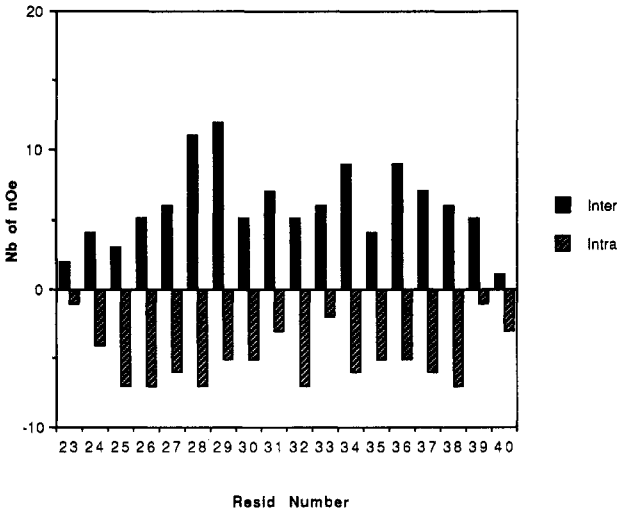

FIGURE 3: Number of distance restraints per residue along the sequence of the peptide 24-41c.

36 is only 1.36 Å. These values confirm that the conformation of the region 28−36 is better defined than the rest of the peptide. This is also consistent with the higher number of interresidue nOes in the region 28−36 (Figure 3).

The region 28−36 of the 10 selected structures, with their backbone heavy atoms (N, Cα, and C) superposed, is shown in Figure 4. In all the structures the distances separating the α-carbons of Arg-30 and Gly-33 is <7 Å. This observation is consistent with the involvement of residues Asp-30−Gly-33 in a reverse turn (Wilmott & Thornton, 1990). The average values of the ϕ and ψ torsion angles for residues 30−33 are reported in Table 4. The ψ value of residue His-31 and the ϕ and ψ of residue Arg-32 are consistent with the geometry of a Type I turn (Willmott & Thornton, 1990). However, the value of the ϕ angle of residue His-31 is −151° (Table 4). It should be noted that the value of −151° is consistent with the observed J_{NH-H_α} for this residue differing from the canonical value of −60°

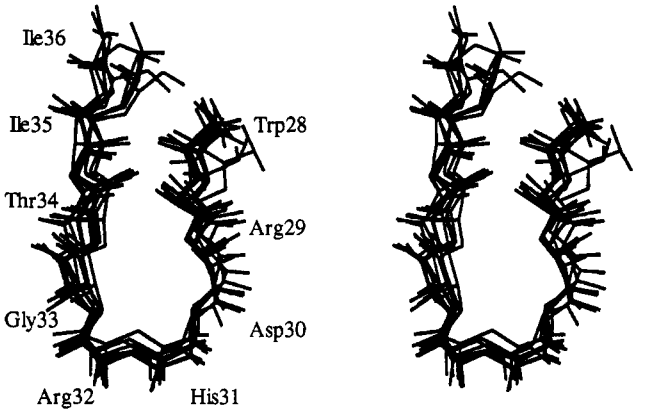

FIGURE 4: Superposition of region 28−36 of the 10 refined structures of the peptide 24-41c fitted on the backbone atoms (N, Cα, C). For clarity only the N, Cα, C, and O atoms are shown.

Table 4: Average Torsion Angles Calculated for the 10 Selected Structures for Residues His-31 and Arg-32 and Corresponding Standard Values for a Type I Turn

	ϕ His-31	ψ His-31	ϕ Arg-32	ψ Arg-32
avTA[a]	−151.1 (±32)	−34 (±16)	−98 (±1.5)	−16 (±20)
Type I TA[a]	−60	−30	−90	0
dNO[b]			2.78 (±0.05)	
aNHO[b]			154.4 (±6.0)	

[a] Torsion angles are given in degrees. The standard deviations are given in parentheses. [b] Average Gly-33 N−Asp-30 Oγ distance (dNO) and Gly-33 N−Gly-33 NH−Asp-30 Oγ) angle (aNHO) calculated for the subset of the 7 refined structures compatible with the existence of a hydrogen bond between Gly-33 NH and Asp-30 Oγ.

for a Type I turn (Table 4). A consequence of this value of ϕ(His-31) is that the orientation of the first peptide plane of the reverse turn (between Asp-30 and His-31) is different from that observed in a standard Type I β turn; in a standard Type I β turn, the carbonyl group of the first peptide bond points inside the turn, whereas in the peptide 24-41c it points outside. As a result the carbonyl oxygen of residue Asp-30 cannot be an acceptor in a hydrogen bond with the Gly-33 NH proton. The side chain of the Asp-30 residue points inside the reverse turn. Among the set of 10 structures selected, 7 are found to be compatible with the existence of a hydrogen bond between the NH proton of residue Gly-33 and the Oγ of residue Asp-30. In this subset of structures, the average distance between the NH proton of Gly-33 and the closest Oγ is 2.78 Å (Table 4). Furthermore, the corresponding average (Gly-33 N, Gly-33 NH, Asp-30 Oγ) angle is 154.1° (Table 4) in good agreement with the J_{NH-H_α} observed for this residue (Bystrov, 1976). These results suggest that the oxygen of the side chain of residue Asp-30 might be an acceptor of a hydrogen bond involving the Gly-33 NH proton.

On the C-terminal side of the reverse turn (region 34−36), the peptide 24-41c exhibits a structured loop that is not a classifiable α or β secondary structure. Another interesting feature of the peptide concerns the positions of the side chains of residues 27, 28, 35, and 36. In the refined structures, Trp-28 was found to be in spatial proximity with Val-27 and either Ile-36 or Ile-35, indicating the presence of a hydrophobic cluster. The region 27−36 of one of the refined structures is shown in Figure 5.

Comparison with the Structure of the Corresponding Region of the Toxin α. The 10 selected structures of the

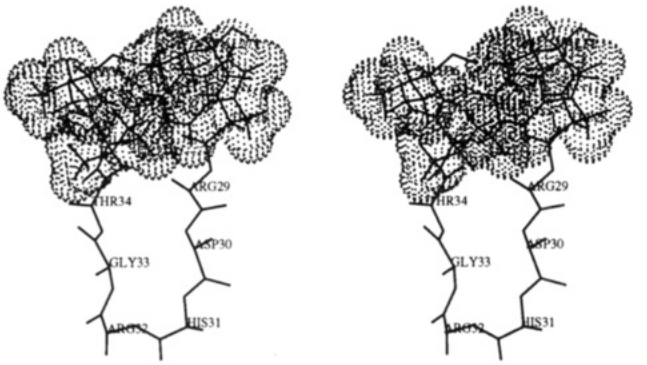

FIGURE 5: Region 27−36 of one of the refined structures of the peptide 24-41c. Only the N, Cα, C, and O atoms are represented except in the case of Val-27, Trp-28, Ile-35, and Ile-36 residues for which all atoms are shown.

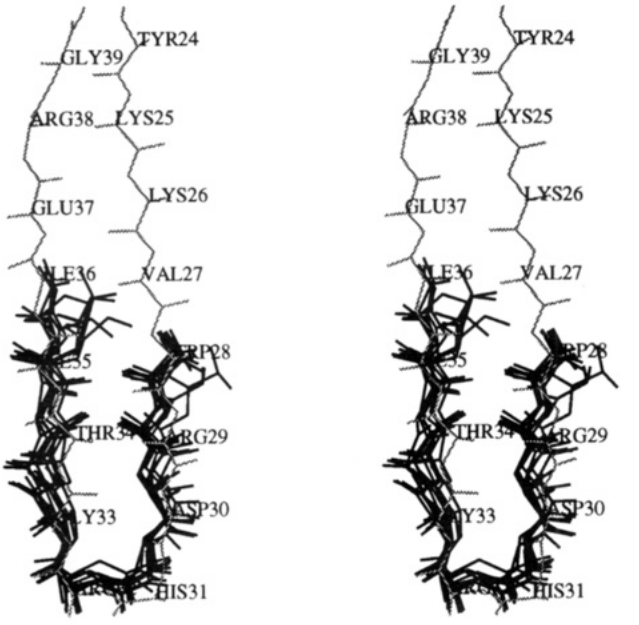

FIGURE 6: Superposition of the 10 refined structures of the peptide 24-41c: (region 28−36) (solid line) together with the loop II of the toxin α (dashed line) fitted on the backbone atoms (N, Cα, and C). For clarity only the N, Cα, C, and O atoms are shown.

peptide (region 28−36) are superimposed with the corresponding region of the toxin α in Figure 6. In the native toxin, the region 24−41 forms a β-hairpin motif consisting of two well-defined β-sheet strands, 23−29 and 34−40, connected by a Type I β turn involving residues 30−33 (Zinn-Justin et al., 1992). No β-sheet was found in the isolated peptide 24-41c. The differences in the Hα chemical shifts between the toxin and peptide are largest in the regions 23−29 and 34−40, with the toxin exhibiting larger downfield shifts than the peptide. This is consistent with the difference in structuring in these regions. Weaker chemical shift differences are found in the reverse turn region in accord with the relative similarity of the toxin and the peptide in the region 30−33. However, for regions 23−29 and 34−40, the presence of the two loops I and III in the native toxin is also likely to contribute to the chemical shift differences.

A detailed comparison of the turn structure in the toxin and in the cyclic peptide reveals significant structural differences. In the toxin, the plane formed by the third amide group of the 30−33 turn is approximately perpendicular to that formed by the backbone atoms of the turn, whereas it is approximately parallel in the peptide. In addition, the first amide plane adopts a canonical orientation in the toxin ($\phi = -60°$), whereas, as previously mentioned, this is $-151°$ in the peptide.

Trp-28 is involved in different hydrophobic packing in the toxin and peptide. In the toxin, the side chains of Trp-28 and Ile-35 are in spatial proximity on the same side of a β-sheet. The side chain of residue Trp-28 does not interact with the side chain of residue Ile-36, which is on the opposite face of the sheet. In the peptide, Trp-28 forms part of a hydrophobic cluster in which the side chain of this residue is in contact with that of Ile-36, as represented in Figure 5.

DISCUSSION

The work presented here provides evidence based on NMR spectroscopy and molecular modeling that, in aqueous solution at pH 5.4 and 276 K, the cyclic peptide 24-41c contains a relatively disordered region and a relatively structured region. The ordered region, involving residues 28−36, contains three structural elements: (i) the tetrapeptide Asp-30, His-31, Arg-32, and Gly-33 organized as a reverse turn, (ii) the segment 33−36 organized as a loop, and (iii) a hydrophobic cluster involving residues Val 27, Trp-28, Ile-35, and Ile-36.

The presence of β-turns in synthetic peptides has been previously documented (Dyson et al., 1985, 1988b, 1990; Williamson et al., 1986; Reed et al., 1988; Delepierre et al., 1990; Blanco et al., 1991; Chandrasekhar et al., 1991) and often involves proline residues. In some cases the reverse turn(s) in peptide fragments in solution have been found to be at somewhat different locations in the sequence than in the parent protein. An example of this is the 12−26 fragment of Tendamistat, which contains a β-turn structure in the native protein at residues 17−20. The fragment contains at least three β-turns, at residues 16−19, 18−21, and 20−23, these structures being in rapid exchange (Blanco et al., 1991). However, examples of turn location conserved in peptide fragments derived from proteins have also been reported. A peptide fragment from actin adopts a reverse turn in trifluoroethanol at the same position as in the parent protein (Sönnichsen et al., 1992). No conformational preference was detected for this peptide in aqueous solution. Turn conservation has also been seen in myoglobin fragments (Shin et al., 1993) and in a fragment of the B1 domain of a G protein (Blanco et al., 1994). In the present case, reversal of the peptide chain occurs at an identical position, 30−33, in aqueous solution and in the parent protein. The folding of the tetrapeptide 30−33 as a turn is due partly to the propensity of the local amino acid sequence (Asp, His, Arg, Gly). Aspartic acid residues have a tendency to occupy position *i* in Type I turns (Baker & Hubbard, 1984), with one of their side-chain oxygens establishing a hydrogen bond with the NH of residue *i* + *3* (Finkelstein et al., 1977; Richardson et al., 1981; Wilmott & Thornton, 1988). Moreover, arginine has a marked tendency to occupy an *i* + *2* position in Type I turns and glycine residues are frequently found at position *i* + *3* of reverse turns.

The present peptide contains a cluster of hydrophobic side chains (Val-27, Trp-28, Ile-35, and Ile-36). There is some evidence that hydrophobic and aromatic interactions can stabilize reverse turns in peptides in aqueous solution and may form initiation sites in protein folding (Dyson & Wright, 1993; Blanco et al., 1994; Yao et al., 1994a,b). Hydrophobic

clusters involving two valines, a tryptophan, and a leucine residue have been found in 63- and 20-residue fragments of the 434 repressor under highly denaturing conditions *i.e.*, 4.2 M urea (Neri et al., 1992). The hydrophobic patch in the present peptide might play a role in stabilizing the reverse turn. The hydrophobic packing is accompanied by the presence of a particular loop structure in the 33−36 segment.

Among the factors that may influence the peptide conformation is the disulfide 24-41. This disulfide was introduced as a conformational constraint to bias the peptide conformational distribution toward that of the native protein. However, the structural analysis does not provide clear indications as to how the disulfide stabilizes the turn, as there is considerable conformational flexibility in the region containing the disulfide. However, in principle one would expect the cyclization to encourage turn formation by eliminating the entropic penalty for chain reversal that is present in the linear peptide. That no β-sheet was detected in the peptide could be related to the absence of the intraprotein stabilizing elements present in the parent toxin. Indeed, several residues of the toxin's β sheet interact with residues present in adjacent loops (Zinn-Justin et al., 1992).

How can we relate the results of the present work to the immunogenic properties of the toxin and the peptide? As discussed in the introduction, it might be expected that, to select B cells producing cross-reactive antibodies, a peptide should share some conformational similarities with the cross-reacting protein. The present results provide experimental evidence substantiating this idea. Indeed, the immunogenic peptide 24-41c in aqueous solution and the cross-reacting toxin both possess turn structures located at equivalent positions. We therefore suggest that the similar structuring of this limited part of the peptide may be partly responsible for the cross-reacting property of the antibodies produced by the selected B cells. In this context, it is of interest to note that a peptide from myohemerythrin, when bound to the antibody B13A2, adopts a conformation resembling that of the corresponding sequence in the native protein (Tsang et al., 1992).

As a caveat to the present results, it can be postulated that the addition of constraints leading to a better conformational mimicry of a given protein region may result in an increase in the affinity of the anti-peptide antibodies for the parent protein. Preliminary studies with the present system using peptides cyclized with additional conformational restraints tend to confirm the validity of this approach (Thomas et al., 1993; Leonetti et al., in press).

ACKNOWLEDGMENT

Dr. Vincent Dive is gratefully acknowledged for stimulating discussions and for numerous tips. We thank Dr. Sophie Zinn-Justin and Dr. Bernard Gilquin for valuable discussions.

REFERENCES

Arnon, R. (1991) *Mol. Immunol. 28*, 209.
Arnon, R., & Sela, M. E. (1969) *Proc. Natl. Acad. Sci. U.S.A. 62*, 163.
Arnon, R., Elchanan, M., Sela, M. E., & Anfisen, C. B. (1971) *Proc. Natl. Acad. Sci. U.S.A. 68*, 1450.
Aue, W. P., Bartholdi, E., & Ernst, R. R. (1976) *J. Chem. Phys. 64*, 2229.
Bahraoui, E. M., Granier, C., Van Rietschoten, J., Rochat, H., & El Ayeb, M. (1986) *J. Immunol. 136*, 3371.
Baker, E. N., & Hubbard, R. E. (1984) *Prog. Biophys. Mol. Biol. 44*, 97.
Bax, A., & Davis, D. G. (1985) *J. Magn. Reson. 63*, 207.
Bax, A., Sklenàr, V., Gronenborn, A. M., & Clore, G. M. (1987) *J. Am. Chem. Soc. 109*, 6511.
Berendsen, H. J. C., Potsma, J. P. M., van Gunsteren, W. F., DiNola, A., & Haak, J. R. (1984) *J. Chem. Phys. 81*, 3684.
Blanco, F. J., Jimenez, M. A., Rico, M., Santoro, J., Herrantz, J., & Nito, J. L. (1991) *Eur. J. Biochem. 200*, 345.
Blanco, F. J., Jimenez, M. A., Herrantz, J., Rico, M., Santoro, J., & Nito, J. L. (1993) *J. Am. Chem. Soc. 115*, 5887.
Blanco, F. J., Rivas, G., & Serrano, L. (1994) *Nature Struct. Biol. 1*, 584.
Bodenhausen, G., Kogler, H., & Ernst, R. R. (1984) *J. Magn. Reson. 58*, 370.
Borras-Cuesta, F., Petit-Carmudan, A., & Fedon, Y. (1987) *Eur. J. Immunol. 17*, 1213.
Bothner-By, A. A., Stephens, R. L., Lee, J., Warren, C. D., & Jeanloz, R. W. (1985) *J. Am. Chem. Soc. 106*, 811.
Brooks, B. R., Bruccoleri, R. E., Olafson, B. D., States, D. J., Swaminathan, S., & Karplus, M. (1983) *J. Comput. Chem. 4*, 187.
Brünger, A. T. (1992) X-PLOR version 3.1, Yale University Press, New Haven, CT, and London.
Brünger, A. T., Kuriyan, J., & Karplus, M. (1987) *Science 235*, 458.
Brüschweiler, R., Roux, B., Blackledge, M., Griesinger, C., Karplus, M., & Ernst, R. R., (1992) *J. Am. Chem. Soc. 114*, 2289.
Bystrov, V. F. (1976) *Prog. Nucl. Magn. Reson. Spectrosc. 10*, 41.
Chandrasekhar, K., Profy, A. T., & Dyson, H. J. (1991) *Biochemistry 30*, 9187.
Delepierre, M., Larvor, M. P., Baleux, F., Djavadi-Ohaniance, L., & Golberg, M. (1990) XIV International Conference on Magnetic Resonance in Biological Systems, Warwick.
DiMarchi, R., Brooke, G., Gale, C., Cracknell, V., Doel, T., & Mowat, N. (1986) *Science 232*, 639.
Dreesman, G. R., Sanchez, Y., Ionescu-Matiu, I., Sparrow, J. T., Six, H. R., Peterson, D. L., Hollinger, F. B., & Melnick, J. L. (1982) *Nature 295*, 158.
Dyson, H. J., & Wright, P. E. (1993) *Curr. Opin. Struct. Biol. 3*, 60.
Dyson, H. J., Cross, K. J., Houghten, R. A., Wilson, I. A., Wright, P. E., & Lerner, R. A. (1985) *Nature 318*, 480.
Dyson, H. J., Rance, M., Houghten, R. A., Wright, P. E., & Lerner, R. A. (1988a) *J. Mol. Biol. 201*, 201.
Dyson, H. J., Lerner, R. A., & Wright, P. E. (1988b) *Annu. Rev. Biophys. Chem. 17*, 305.
Dyson, H. J., Satterthwhait, A. C., Lerner, R. A., & Wright, P. E. (1990) *Biochemistry 29*, 7828.
Felix 2.1 (1993) Biosym Technologies, 9685 Scranton Rd., San Diego, CA 92121-2777.
Finkelstein, A. V., Ptitsyn, O. B., & Kozitsyn, S. A. (1977) *Biopolymers 16*, 497−523.
Francis, M. J., Hastings, G. Z., Syred, A. D., Mac Ginn, B., Brown, F., & Rowlands, D. J. (1987) *Nature 300*, 168.
Good, M. F., Maloy, W. L., Lunde, M. N., Margalit, H., Cornette, J. L., Smith, G. L., Moss, B., Miller, L. H., & Berzofsky, J. A. (1987) *Science 235*, 1059.
Goodman, E. M., & Kim, P. S. (1989) *Biochemistry 28*, 4343.
Jemmerson, R. (1987) *Proc. Natl. Acad. Sci. U.S.A. 84*, 9180.
Karplus, M. (1959) *J. Phys. Chem. 30*, 11.
Leclerc, C., Przewlocki, G., Schultze, M. P., & Chedid, L. (1987) *Eur. J. Immunol. 17*, 1213.
Léonetti, M., Pillet, L., Maillère, B., Lamthang, H., Frachon, P., Couderc, J., & Ménez, A. (1990) *J. Immunol. 145*, 4214.
Lerner, R. A. (1982) *Nature 299*, 592.
Lerner, R. A., Niram, H. L., Houghten, R. A., Walker, L. E., Reisfield, R. A., & Wilson, I. A. (1984) *Adv. Immunol. 36*, 1.
Marion, D., & Wüthrich, K. (1983) *Biochem. Biophys. Res. Commun. 113*, 967.
Neri, D., Billeter, M., Wider, G., & Wuthrich, K. (1992) *Science 257*, 1559.
Nilges, M., Clore, M., & Gronenborn, A. M. (1988) *FEBS Lett. 239*, 129.
Palmenberg, A. (1987) *Nature 329*, 668.
Plateau, P., & Gueron, M. (1982) *J. Am. Chem. Soc. 104*, 7310.

Reed, J., Hull, W. E., Lieth, C. W., Kübler, D., Subaï, S., & Kinzel, V. (1988) *Eur. J. Biochem. 178*, 141.
Richardson, J. S. (1981) *Adv. Protein Chem. 34*, 167.
Rico, M., Nieto, J. L., Santoro, J., Bermejo, F. J., Herrantz, J., & Gallego, E. (1983) *FEBS Lett. 162*, 314.
Roy, S., Scherer, M. T., Briner, T. J., Smith, J. A., & Gefter, M. L. (1989) *Science 244*, 572.
Shin, H.-C., Merutka, G., Waltho, J. P., Wright, P. E., & Dyson, H. J. (1993) *Biochemistry 32*, 6348.
Sönnichsen, F. D., Van Eyck, J. E., Hodges, R. s., & Sykes, B. D. (1992) *Biochemistry 31*, 8790.
States, D. J., Haberkorn, R. A., & Ruben, D. J. (1982) *J. Magn. Reson. 48*, 286.
Steward, M. W., & Howard, C. R. (1987) *Immunol. Today 8*, 51.
Sybyl (1994) Tripos Associates, Inc., 1699 S. Hanley Rd., Suite 303, St. Louis, MO 63144-2913.
Thomas, A., Roux, B., & Smith, J. C. (1993) *Biopolymers 33*, 1249.
Trémeau, O., Boulain, J. C., Couderc, J., Fromageot, P., & Ménez, A. (1986) *FEBS Lett. 208*, 236.
Tsang, P., Rance, M., Fieser, T. M., Ostresh, J. M., Houghten, R. A., Lerner, R. A., & Wright, P. E. (1992) *Biochemistry 31*, 3862.
Williamson, M. P., Hall, M. J., & Handa, B. K. (1986) *Eur. J. Biochem. 158*, 527.
Wilmot, C. M., & Thornton, J. M. (1988) *J. Mol. Biol. 203*, 221.
Wilmot, C. M., & Thornton, J. M. (1990) *Protein Eng. 3*, 479.
Wright, P. E., Dyson, H. J., & Lerner, R. A. (1988) *Biochemistry 27*, 7167.
Wüthrich, K., (1986) *NMR of Proteins and Nucleic Acids*, Wiley-Interscience Publications, New York.
Wüthrich, K., Billeter, M., & Braun, W. (1983) *J. Mol. Biol. 169*, 949.
Yao, J., Dyson, H. J., & Wright, P. E. (1994a) *J. Mol. Biol. 243*, 754.
Yao, J., Feher, V. A., Fabiola Espejo, F., Reymond, M. T., Wright, P. E., & Dyson, H. J. (1994b) *J. Mol. Biol. 243*, 736.
Zinn-Justin, S., Roumestand, C., Gilquin, B., Bontems, F., Ménez, A., & Toma, F. (1992) *Biochemistry 31*, 11335.

BI950145W